RadioGraphics

CT of Internal Hernias[1]

Nobuyuki Takeyama, MD • Takehiko Gokan, MD • Yoshimitsu Ohgiya, MD • Shuichi Satoh, MD • Takashi Hashizume, MD • Kiyoshi Hataya, MD • Hiroshi Kushiro, MD • Makoto Nakanishi, MD • Mitsuo Kusano, MD • Hirotsugu Munechika, MD

CME FEATURE

See accompanying test at http://www.rsna.org/education/rg_cme.html

LEARNING OBJECTIVES FOR TEST 4

After reading this article and taking the test, the reader will be able to:

- Describe the normal anatomy of the peritoneal cavity and the characteristic anatomic location of each type of internal hernia.
- Identify the characteristic CT appearances of various types of internal hernias.
- Discuss the clinical findings and appropriate management of internal hernias.

Computed tomography (CT) plays an important role in diagnosis of acute intestinal obstruction and planning of surgical treatment. Although internal hernias are uncommon, they may be included in the differential diagnosis in cases of intestinal obstruction, especially in the absence of a history of abdominal surgery or trauma. CT findings of internal hernias include evidence of small bowel obstruction (SBO); the most common manifestation of internal hernias is strangulating SBO, which occurs after closed-loop obstruction. Therefore, in patients suspected to have internal hernias, early surgical intervention may be indicated to reduce the high morbidity and mortality rates. In a study of 13 cases of internal hernias, nine different types of internal hernias were found and the surgical and radiologic findings were correlated. The following factors may be helpful in preoperative diagnosis of internal hernias with CT: *(a)* knowledge of the normal anatomy of the peritoneal cavity and the characteristic anatomic location of each type of internal hernia; *(b)* observation of a saclike mass or cluster of dilated small bowel loops at an abnormal anatomic location in the presence of SBO; and *(c)* observation of an engorged, stretched, and displaced mesenteric vascular pedicle and of converging vessels at the hernial orifice.

Abbreviations: PDH = paraduodenal hernia, SBO = small bowel obstruction

RadioGraphics 2005; 25:997–1015 • **Published online** 10.1148/rg.254045035 • **Content Codes:** CT GI

[1]From the Departments of Radiology (N.T., T.G., Y.O., T.H., H.M.) and General and Gastrointestinal Surgery (M.K.), Showa University School of Medicine, 1-5-8 Hatanodai, Shinagawa-ku, Tokyo 142-8666, Japan; the Departments of Radiology (S.S.) and Surgery (K.H.), Yokohama Asahi Chuo General Hospital, Yokohama, Japan; the Department of Surgery, Kikuna Memorial Hospital, Yokohama, Japan (H.K.); and the Department of Surgery, Totsuka Kyouritsu Hospital, Yokohama, Japan (M.N.). Recipient of a Certificate of Merit award for an education exhibit at the 2003 RSNA Annual Meeting. Received March 12, 2004; revision requested April 8; final revision received September 30; accepted October 5. All authors have no financial relationships to disclose. **Address correspondence to** N.T. (e-mail: *momiji@mtc.biglobe.ne.jp*).

Types of Internal Hernias and Their Relative Frequencies

Type of Hernia	Relative Frequency (%)
Foramen of Winslow	8
Paraduodenal (left and right)	53
Transmesenteric	8
Transomental	1–4
Pericecal	13
Intersigmoid	6
Supravesical and pelvic*	6†

*Pelvic hernias include hernias through the broad ligament, perirectal fossa, and fossa of Douglas.
†The relative frequency of hernia through the broad ligament is 4%–5%.

Introduction

Internal hernias involve protrusion of the viscera through the peritoneum or mesentery and into a compartment in the abdominal cavity. The most common presentation is an acute intestinal obstruction of small bowel loops that develops through normal or abnormal apertures (1,2). The responsible hernial orifices are usually preexisting anatomic structures, such as foramina, recesses, and fossae. Pathologic defects of the mesentery and visceral peritoneum, which are caused by congenital mechanisms, surgery, trauma, inflammation, and circulation, are also potential herniation orifices (3,4).

Preoperative diagnosis is difficult because clinical symptoms may range from intermittent and mild digestive complaints to acute-onset intestinal obstruction. Internal hernias are silent if they are easily reducible, but the majority often cause epigastric discomfort, periumbilical pain, and recurrent episodes of intestinal obstruction (3,5). Internal hernias are clinically apparent only when incarcerated internal hernias result from small bowel obstruction (SBO); therefore, a delay in diagnosis may lead to strangulation and an increased risk of serious complications.

We categorized various internal hernias and potential orifices with relative frequency (Table) on the basis of their topographic distribution in the peritoneal cavity (Figs 1, 2) according to the classification of Welch (8).

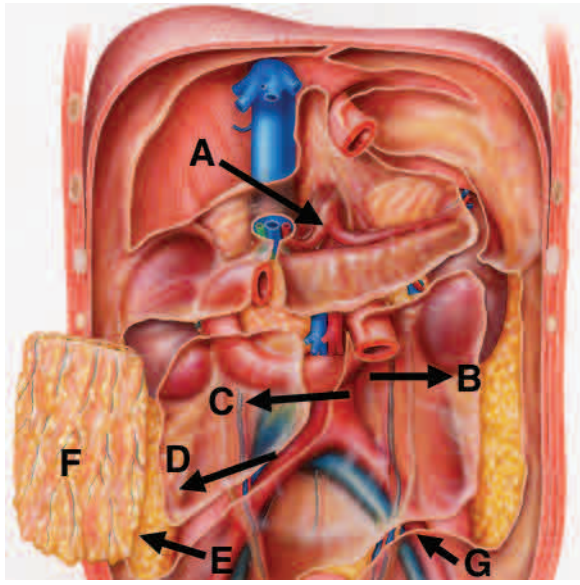

Figure 1. Drawing (coronal view) shows the locations and directions of internal hernias of the upper and lower abdominal peritoneal cavity. *A* = foramen of Winslow hernia, *B* = left paraduodenal hernia, *C* = right paraduodenal hernia, *D* = transmesenteric hernia, *E* = pericecal hernia, *F* = transomental hernia, *G* = intersigmoid hernia. (Adapted and reprinted, with permission, from reference 6.)

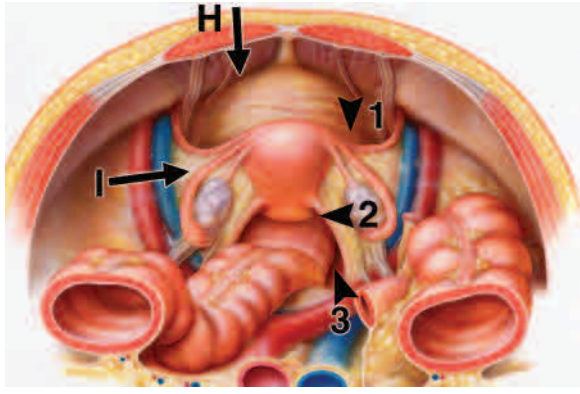

Figure 2. Drawing (superior view) shows the locations of internal hernias, pouches, and fossae of the pelvic cavity in a female patient. *H* = supravesical hernia, *I* = hernia through the broad ligament, *1* = vesicouterine pouch, *2* = Douglas (rectouterine) pouch, *3* = perirectal fossa. (Adapted and reprinted, with permission, from reference 7.)

In this article, we describe our clinical experience with internal hernias, the imaging technique, and diagnosis with computed tomography (CT), including the CT findings and their clinical rel-

evance as well as the important role of multi–detector row CT. We then discuss the locations and relative frequencies of internal hernias, which include foramen of Winslow, paraduodenal, transmesenteric, transomental, pericecal, sigmoid mesocolon, and supravesical and pelvic hernias.

In the sections on internal hernias, we describe the anatomic locations and embryologic features of potential hernial orifices (foramina, fossae, recesses, defects of the mesentery and visceral peritoneum) and the clinical, surgical, and radiologic findings, including the characteristic CT appearances. We also present CT images, some surgical results, and some intraoperative photographs. Finally, we briefly describe the management of internal hernias.

Clinical Experience

From November 1995 to February 2004, a retrospective review of medical records and radiologic images revealed 13 patients (eight male, five female) with surgically proved internal hernias at our institution and branch hospitals. Their age ranged from 12 to 86 years (mean age, 56.1 years) with more than half of the patients over age 50 years. All patients except one with clinical and radiologic findings suggestive of acute intestinal obstruction underwent single detector row CT of the abdomen and pelvis at the time of admission. One patient underwent CT 4 days after conservative treatment. Four patients with low-grade obstruction underwent enteroclysis, which is particularly helpful in depicting and grading the severity of partial obstruction and demonstrating sites of incomplete obstruction.

CT examinations were performed with the following imaging units: ProSeed SA (GE Healthcare Technologies, Waukesha, Wis) ($n = 7$); Hi-speed DXI (GE Healthcare Technologies) ($n = 1$); TCT-700S (Toshiba, Tokyo, Japan) ($n = 1$); TCT-60A (Toshiba) ($n = 2$); and SCT-7000 (Shimadzu, Kyoto, Japan) ($n = 2$).

The duration of symptoms before hospital admission ranged from as little as 3 hours to as long as 3 months. The interval between CT examination at the time of admission and surgery ranged from 2 hours to 20 days. Six patients underwent emergency operations within 7 hours of CT examination. Four patients were treated conservatively with insertion of a nasogastric tube or a long intestinal tube to drain the intestinal fluid, but these patients underwent operations within 12–42 hours of CT examination because of aggravated symptoms. The remaining three patients underwent operations within 4–20 days after CT examinations because at first they were making good progress with conservative treatment by means of nasogastric or long intestinal tube decompression, but their symptoms became aggravated little by little.

During laparotomy in each patient, reduction of the hernia contents, resection of necrotic bowel loops, and primary anastomosis (enterostomy in one case) were performed. Gangrenous changes in the incarcerated bowel loops were present in seven patients, and six patients had viable bowel loops. Eleven patients had no history of abdominal surgery or trauma. Only two patients had a history of appendectomy.

Nonspecific abdominal symptoms of intestinal obstruction were observed in all 13 patients. These included some degree of epigastric pain, abdominal pain, tenderness, abnormal bowel sounds, nausea, vomiting, and palpation of a mass.

Imaging Technique

Gastrointestinal studies enhanced with intraluminal contrast material (barium-enhanced studies, enteroclysis) and abdominal CT enable accurate diagnosis of any type of internal hernia (9,10). In mechanical high-grade SBO, small bowel follow-through study has a limitation in emergency use. Enteroclysis can be performed more quickly and has been shown to have high accuracy in the evaluation of SBO, but is contraindicated in patients with high-grade closed-loop obstruction and in those with suspected hernial strangulation (11). Recently, CT has demonstrated the importance of preoperative diagnosis of early or partial obstruction and closed-loop obstruction.

In our CT examination, intravenous administration of contrast material is essential to determine the cause of obstruction and identify any associated hernial strangulation. All patients except one underwent CT performed with 100 mL of contrast material administered intravenously at a rate of 1–2 mL/sec. The delay between the start of injection and imaging varied between 70 and 90 seconds. All images were acquired with 7–10-mm collimation and a pitch of 1.2–1.5.

One patient underwent nonenhanced CT because she was allergic to the contrast material; CT images clearly demonstrated the presence of strangulating bowel loops as diffuse mesenteric fluid and haziness.

Because of the difficulty of preoperative CT diagnosis, multi–detector row CT may play an important role. Currently, multi–detector row technology provides substantial improvements in the quality of two- and three-dimensional reformatted images, which have evolved in addition to the axial images. Many images obtained with multi–detector row CT are interpreted at workstations by manually paging up and down or reformatting by means of high-quality three-dimensional reformation techniques, such as multiplanar reformation (MPR), shaded surface display (SSD), volume rendering (VR), and maximum intensity projection (MIP).

Multi–detector row CT with three-dimensional reformatting at a workstation provides important advantages over conventional imaging methods in evaluation of the small intestine and surrounding structures (mesentery, mesenteric vasculature, and peritoneal cavity). Multi–detector row CT can play a more active role in identification of the site, level, and cause of SBO, including internal hernias (12,13).

Oral administration of contrast material and water is not necessary in view of the patients' severe condition because intraluminal fluid collected within an SBO segment already serves as a natural contrast agent, demonstrating the bowel wall clearly (12,13). On the other hand, multi–detector row CT coupled with administration of water and oral contrast material allows the diagnosis of SBO. Some investigators advocate use of CT enteroclysis, which provides a flexible method of viewing SBO (14).

Diagnosis of Internal Hernias with CT

Because clinical diagnosis of internal hernias is difficult, imaging studies may play an important role if accurate and reliable CT findings can be obtained. However, CT evaluation of any type of internal hernia is rare in the radiology literature, except for a few reports on paraduodenal and transmesenteric hernias.

The most common internal hernia is strangulating SBO, which occurs after a closed-loop obstruction. CT findings of internal hernias include evidence of SBO. To diagnose the hernial strangulation, many researchers stress the importance of observing the configuration of the obstructed loop, mesenteric changes, and the enhancement patterns of the bowel wall (15–19). In this article, we evaluate two characteristic CT findings: bowel configuration and mesenteric changes. The former consists of a saclike mass or cluster of dilated bowel loops. The latter consists of a mesenteric vascular pedicle that is engorged, stretched, and displaced; in addition, the dilated bowel loops have converging vessels at the entrance of the hernial orifice, thus revealing the impaired venous drainage and continuous influx of the arterial flow (1,3,9,10,15–19).

Locations and Relative Frequencies of Internal Hernias

The occurrence of abdominal internal hernias is rare. They are reported in 0.2%–0.9% of autopsies (2) and in 0.5%–4.1% of cases of intestinal obstruction (3,8,20). The locations and relative frequencies of internal hernias are as follows: paraduodenal, 53%; pericecal, 13%; foramen of Winslow, 8%; transmesenteric and transmesocolic, 8%; pelvic and supravesical, 6%; sigmoid mesocolon, 6%; and transomental, 1%–4% (1–3,20,21).

Foramen of Winslow Hernia

Anatomy

The lesser sac and the greater peritoneal cavity communicate through the epiploic foramen of Winslow. This potential opening is a 3-cm vertical slit situated beneath the upper part of the right border of the lesser sac, cephalad to the duodenal bulb and deep to the liver (Fig 1, *A*). This foramen is located anterior to the inferior vena cava and posterior to the hepatoduodenal ligament, including the portal vein, common bile duct, and hepatic artery (1–3,22).

Features

Foramen of Winslow hernias make up 8% of all internal hernias (1–3). The intestinal segment most commonly involved is the small intestine (60%–70%). The terminal ileum, cecum, and

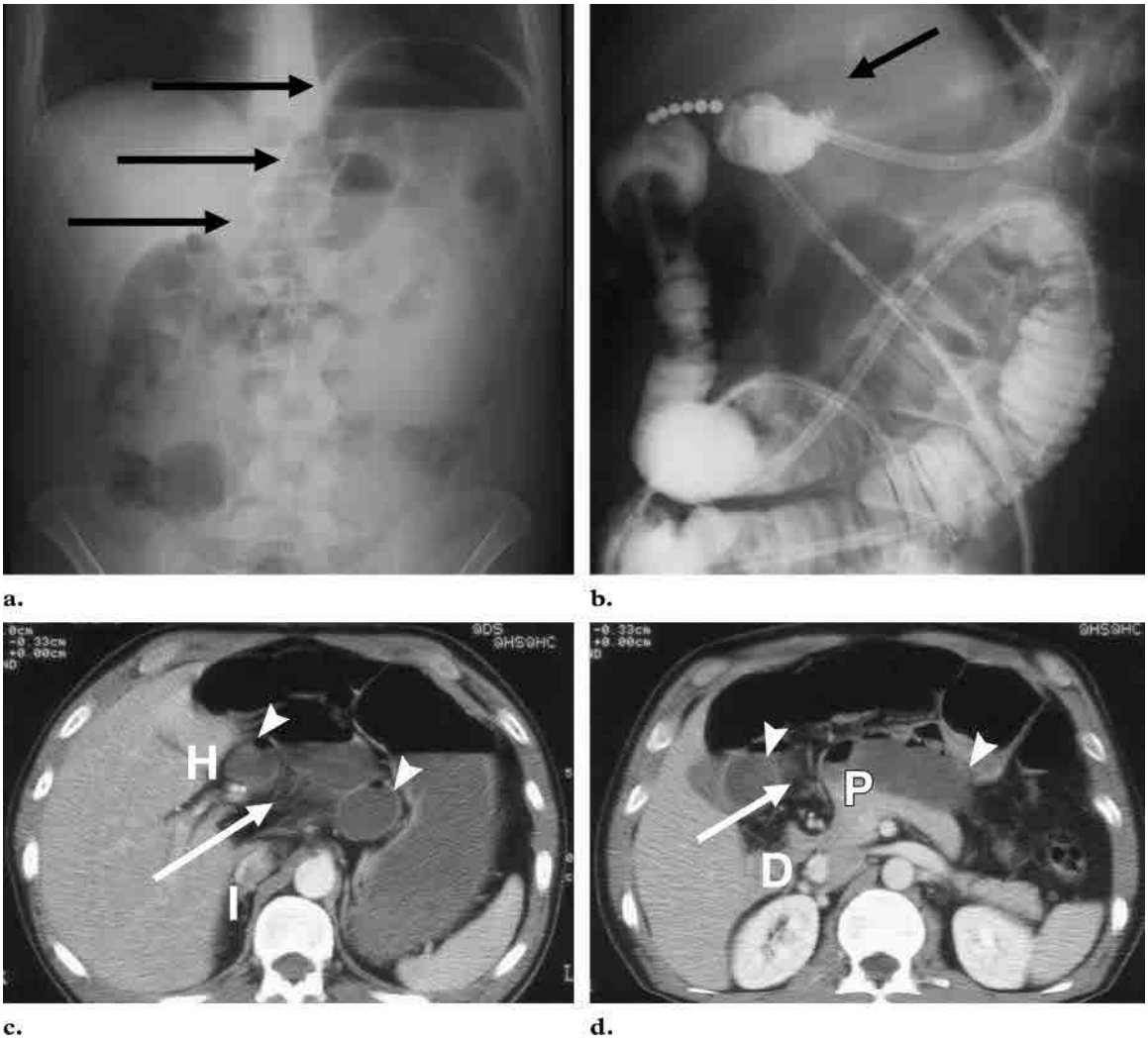

Figure 3. Foramen of Winslow hernia in a 45-year-old man with acute epigastric pain of 18 hours duration. **(a)** Abdominal radiograph shows gas-containing small bowel loops (arrows) in the center of the upper abdomen between the liver and the gastric air bubble. **(b)** Image obtained with enteroclysis performed through a long intestinal tube shows an SBO at the right hepatic flexure (arrow). **(c)** Contrast-enhanced CT scan of the upper abdomen shows the cluster of dilated small bowel loops (arrowheads) in the lesser sac. There are stretched and converging mesenteric vessels (arrow) between the portal vein in the hepatoduodenal ligament *(H)* and the inferior vena cava *(I)*. **(d)** CT scan obtained at the level of the pancreatic head shows crowded mesenteric vessels from the superior mesenteric vein (arrow) between the ascending portion of the duodenum *(D)* and the pancreatic head *(P)*. Arrowheads = small bowel loops. At laparotomy performed 31 hours after CT, adhesion between the gastrocolic ligament and the transverse mesocolon was found. Approximately 50 cm of ileum, located 200 cm from the ligament of Treitz, was herniated into the lesser sac. The herniated ileal loops demonstrated only congestive changes without gangrene.

ascending colon are involved at a rate of about 25%–30% (1,2). Hernias involving the transverse colon, omentum, and gallbladder are rare, although some have been reported in the literature. Predisposing factors include an enlarged foramen of Winslow and excessively mobile intestinal loops due to a long mesentery or persistence of the ascending mesocolon and an ascending colon that is not fused to the parietal peritoneum (1–4,23–26).

Characteristic plain radiographic findings are gas-containing intestinal loops high in the abdomen and medial and posterior to the stomach associated with SBO (Fig 3). The cecum and ascending colon may be absent from their usual locations if they are part of the herniated viscera. Barium-enhanced radiography of the small intestine shows dilatation of bowel loops and usually

reveals the obstruction at the right upper abdomen. Narrowing or obstruction at the hepatic flexure may be visualized with barium enema examination if the hernia involves the cecum and ascending colon (23). The following are the characteristic CT appearances: *(a)* presence of mesentery between the inferior vena cava and main portal vein, *(b)* an air-fluid collection in the lesser sac with a beak directed toward the foramen of Winslow, *(c)* absence of the ascending colon in the right gutter, and *(d)* two or more bowel loops in the high subhepatic spaces (1–3,24–26).

Paraduodenal Hernia

Anatomy

Paraduodenal fossae originate as congenital peritoneal anomalies owing to failure of mesenteric fusion with the parietal peritoneum and an associated abnormal rotation during imprisonment of the small intestine beneath the developing colon (1–3,22,27–33).

In the past, nine different fossae in the vicinity of the duodenum have been described, but clinically just five fossae are important: the superior duodenal fossa, inferior duodenal fossa (fossa of Treitz), paraduodenal fossa (fossa of Landzert), intermesocolic fossa (fossa of Broesike), and mesentericoparietal fossa (fossa of Waldeyer) (27,28). Figure 4 shows the locations of these fossae and their frequencies at autopsy. The fossa of Landzert, present in about 2% of autopsies, is recognized as inducing left paraduodenal hernia (PDH). The fossa of Waldeyer, present in about 1% of autopsies, is recognized as inducing right PDH (22).

Features

PDHs constitute approximately 53% of all internal hernias. Approximately three-fourths of these hernias occur on the left and are more predominant in men than in women, with a ratio of about 3:1 (1–3).

Left PDH develops through the fossa of Landzert into the descending mesocolon and left of the transverse mesocolon and results from failure of fusion of the inferior mesentery to the parietal peritoneum (29). The fossa of Landzert is located at the duodenojejunal junction, which is a zone of

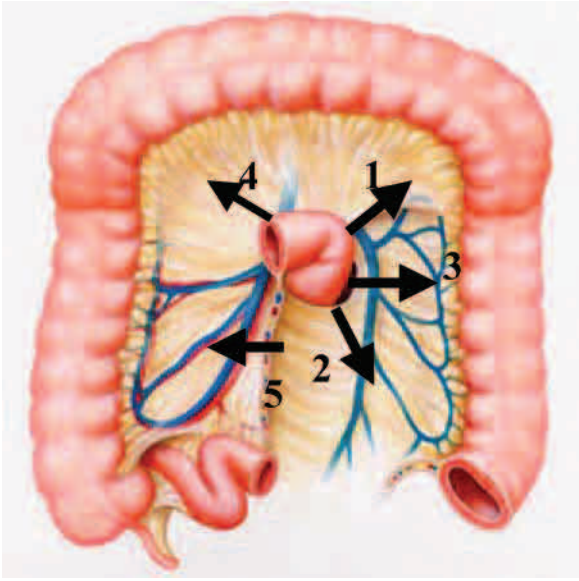

Figure 4. Drawing (coronal view) shows the locations of duodenal fossae. Arrows indicate the directions of hernias through these fossae. The frequency with which each fossa is found at autopsy is given in parentheses. *1* = superior duodenal fossa (50%), *2* = inferior duodenal fossa (fossa of Treitz) (75%), *3* = paraduodenal fossa (fossa of Landzert) (2%), *4* = intermesocolic fossa (fossa of Broesike), *5* = mesentericoparietal fossa (fossa of Waldeyer) (1%). (Adapted and reprinted, with permission, from reference 6.)

confluence of the descending mesocolon, transverse mesocolon, and small bowel mesentery (30). The herniated small bowel loops may become entrapped within this mesenteric sac. The characteristic CT appearance consists of an abnormal cluster or saclike mass of dilated small bowel loops lying between the pancreas and stomach to the left of the ligament of Treitz (Fig 5). There is usually mass effect that displaces the posterior wall of the stomach, the duodenal flexure inferiorly, and the transverse colon inferiorly (30,31). The mesenteric vessels that supply the herniated small bowel segments are crowded, engorged, and stretched at the entrance of the hernial sac (Fig 6) (9,10). Because the anterior wall of the sac contains the inferior mesenteric vein and left colic artery, CT demonstrates these vessels as a landmark above the encapsulated bowel loops.

Right PDH involves the fossa of Waldeyer, which is located immediately behind the superior mesenteric artery and inferior to the transverse segment of the duodenum with or without rotation

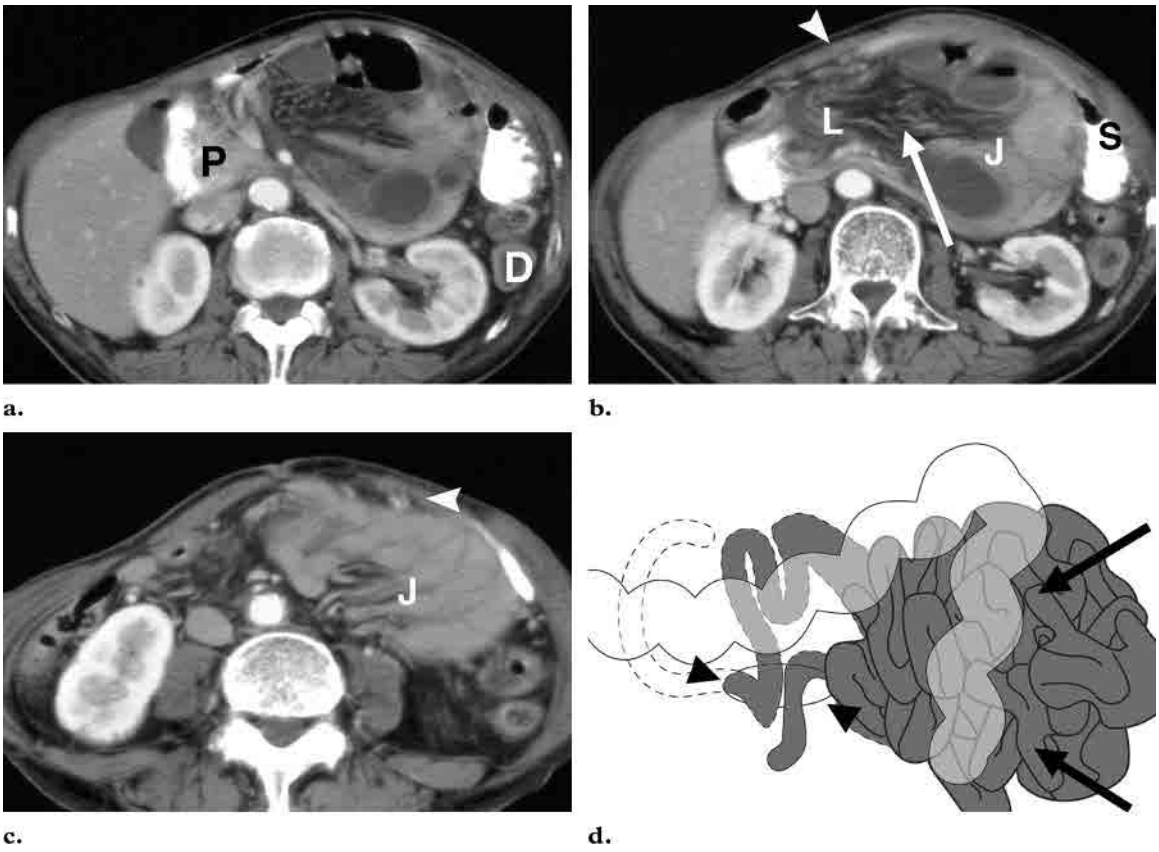

Figure 5. Left PDH in a 72-year-old man with acute, intermittent epigastric pain of 24 hours duration. **(a)** Contrast-enhanced CT scan of the upper abdomen shows a saclike mass of dilated jejunal loops between the pancreatic head *(P)* and stomach. The descending mesocolon *(D)* and stomach are displaced laterally. The dilated inferior mesenteric vein is located at the anterior border of the encapsulated loops. **(b)** CT scan obtained 20 mm below **a** shows crowded and engorged mesenteric vessels (arrow) at the fossa of Landzert *(L)*. *J* = jejunal loops, *S* = stomach, arrowhead = inferior mesenteric vein. **(c)** CT scan of the midabdomen shows the inferior mesenteric vein (arrowhead). This vessel is a landmark for the inferior mesocolon, which is located at the anteromedial border of the encapsulated jejunal loops *(J)*. **(d)** Diagram (coronal view) of the surgical findings shows that the fossa of Landzert is 4 cm in diameter (arrowheads). At laparotomy performed 42 hours after CT, approximately 200 cm of viable jejunum was found (arrows).

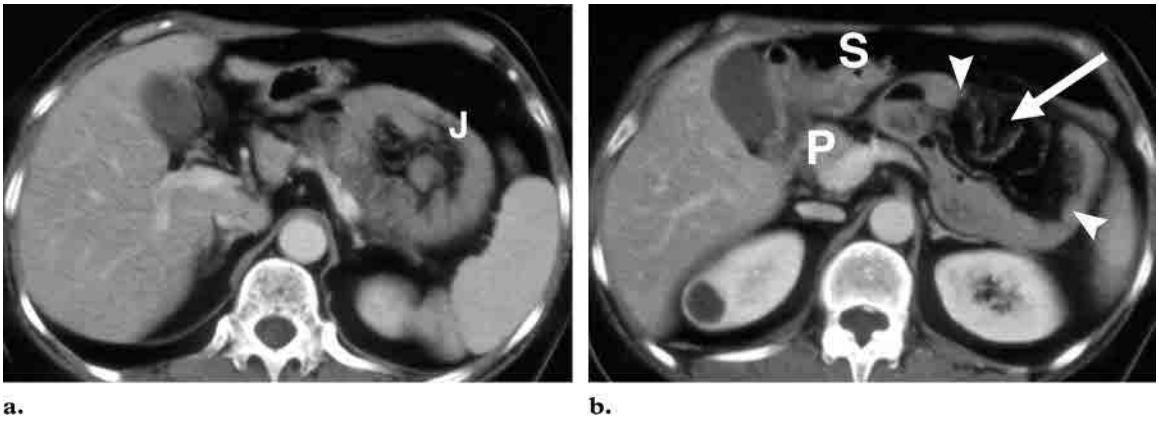

Figure 6. Left PDH in a 55-year-old woman who experienced aggravated epigastric pain followed by 3 months of frequent and intermittent pain. **(a)** Contrast-enhanced CT scan of the upper abdomen shows a saclike mass of proximal jejunal loops *(J)*. In this case, CT did not show the inferior mesenteric vein, which is a landmark for left PDH. **(b)** CT scan obtained 30 mm below **a** shows a horseshoelike configuration of collapsed jejunal loops (arrowheads) and dilated mesenteric vessels (arrow) between the pancreas *(P)* and stomach *(S)* without mass effect. At laparotomy performed 7 hours after CT, the herniated jejunal loops were viable with no gangrene.

Figure 7. Right PDH in a 31-year-old man with sudden onset of severe diffuse abdominal pain. **(a)** Contrast-enhanced CT scan of the upper abdomen shows a saclike mass of fluid-filled bowel loops *(S)*, most of which were jejunal and proximal ileal loops. **(b)** CT scan obtained 30 mm below **a** shows the encapsulated bowel loops herniated through the fossa of Waldeyer *(W)*, which is located behind the superior mesenteric artery (arrowhead) just below the transverse portion of the duodenum *(D)*. *I* = ileal loops. **(c)** CT scan of the lower abdomen shows the superior mesenteric artery (arrowhead), which is displaced anteriorly by the entrapped bowel loops. Dilated and converging vessels (arrows) are seen in the mesentery; dilated ileal loops *(I)* are seen in the left midabdomen. **(d)** Diagram (coronal view) of the surgical findings shows that the fossa of Waldeyer (light gray area) is 10 cm in diameter. At laparotomy performed 2 hours after CT, 350 cm of strangulated small intestine, located 70 cm from the ligament of Treitz, was found. Because the withdrawn bowel loops were purple, jejunostomy was performed without resection.

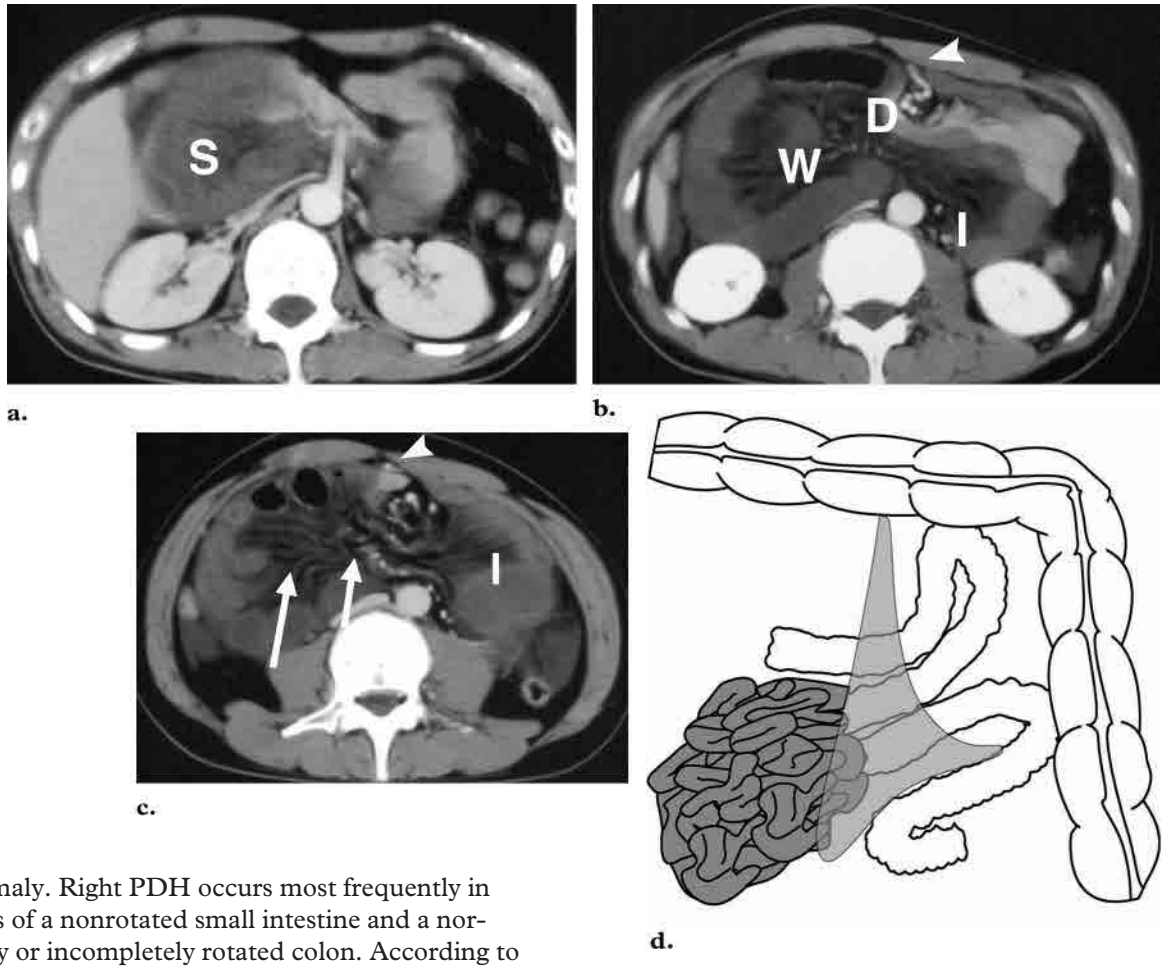

anomaly. Right PDH occurs most frequently in cases of a nonrotated small intestine and a normally or incompletely rotated colon. According to the extent of malrotation, right PDH is associated with location of the superior mesenteric vein to the left of, and ventral to, the superior mesenteric artery and with absence of the normal horizontal duodenum. Because the fossa of Waldeyer extends to the right and downward, directly in front of the posterior parietal peritoneum, right PDH develops into the ascending mesocolon with a right colic vein anteriorly. The superior mesenteric artery and right colic vein are located at the anterior-medial border of the encapsulated small bowel loops and are a landmark for right PDH (Fig 7) (30).

Transmesenteric Hernia

Anatomy

The small bowel mesentery is a broad, fan-shaped fold of peritoneum that suspends the loops of the small intestine from the posterior abdominal wall (1,22). The two layers of peritoneal reflection form the mesentery, which extends from its origin at the ligament of Treitz to the right toward the ileocecal valve (Fig 1, *D*).

Nearly 35% of transmesenteric hernias occur during the pediatric period and are probably caused by a congenital mechanism. Mesenteric defects are usually 2–5 cm in diameter and are

Figure 8. Transmesenteric hernia in a 36-year-old woman with lower abdominal pain of 10 days duration. She was treated conservatively for 20 days by means of decompression with a nasogastric tube or long intestinal tube, intravenous fluids, and antibiotics because of an undiagnosed SBO. However, the SBO developed despite treatment. **(a)** Contrast-enhanced CT scan of the midabdomen shows dilated and fluid-filled small bowel loops *(S)* and crowded and stretched vessels (arrow). **(b)** CT scan of the pelvis shows crowded and converging vessels (arrow) at the hernial orifice. **(c)** Image obtained with enteroclysis performed through the intestinal tube shows the SBO (arrow). **(d)** Diagram (coronal view) of the surgical findings shows that approximately 180 cm of strangulated ileum (arrows), located 5 cm from the ileocecal valve, was herniated through the mesenteric defect (arrowheads). At laparotomy, a segment of gangrenous ileum was resected. **(e)** Intraoperative photograph shows the hernial orifice, which is oval and 4 cm in diameter.

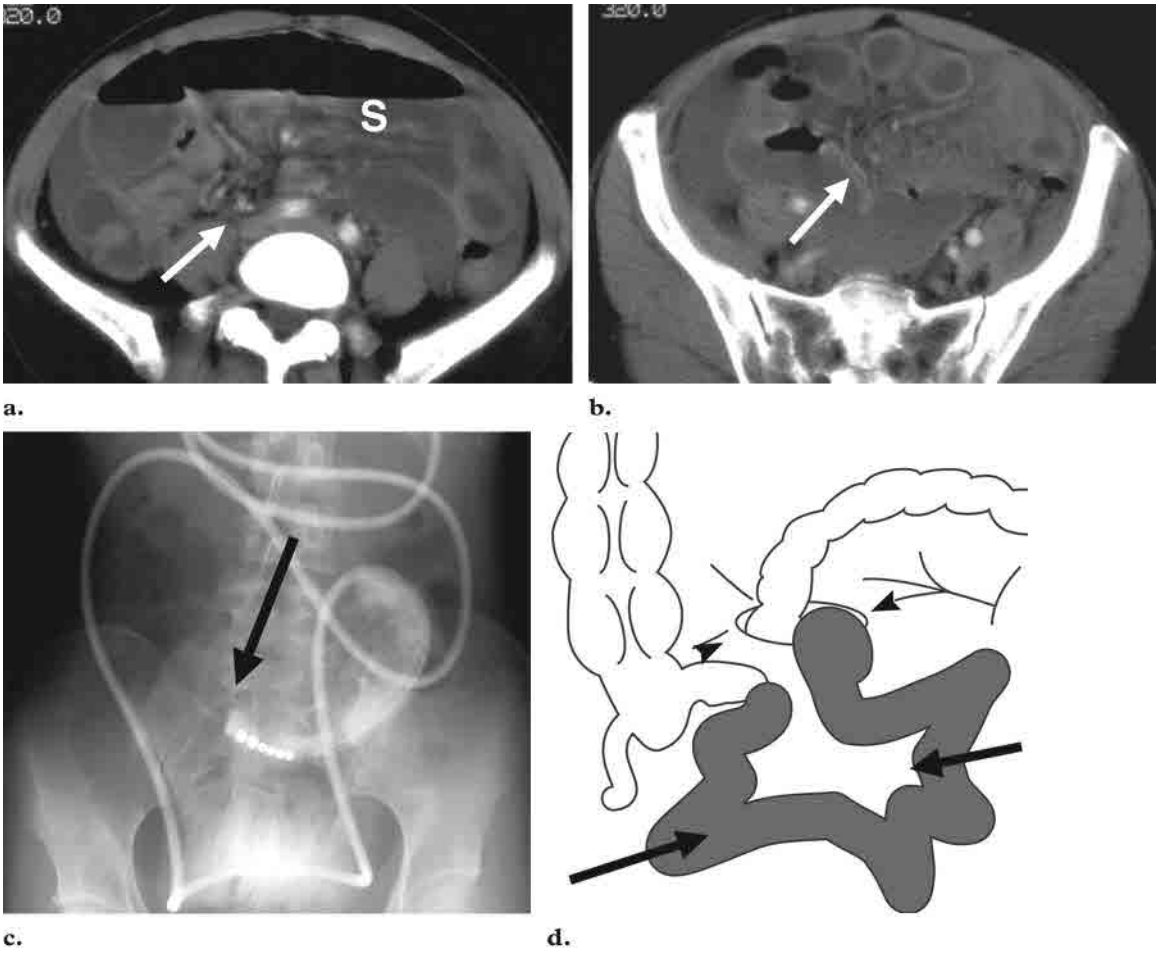

located close to the ligament of Treitz or the ileocecal valve (2,3). Three etiologic hypotheses have been proposed for congenital mesenteric defects: *(a)* partial regression of the dorsal mesentery, *(b)* fenestration during the developmental enlargement of an inadequately vascularized area, and *(c)* an ileocecal mesentery with considerable and rapid lengthening in fetal life (32). In adults, most mesenteric defects are probably the result of surgery, trauma, or inflammation.

Features

Transmesenteric and transmesocolic hernias account for 8% of all internal hernias (1–3). Because of the absence of a limiting hernial sac, mechanical SBO usually occurs in cases of transmesenteric hernia (Fig 8), and it is impossible to

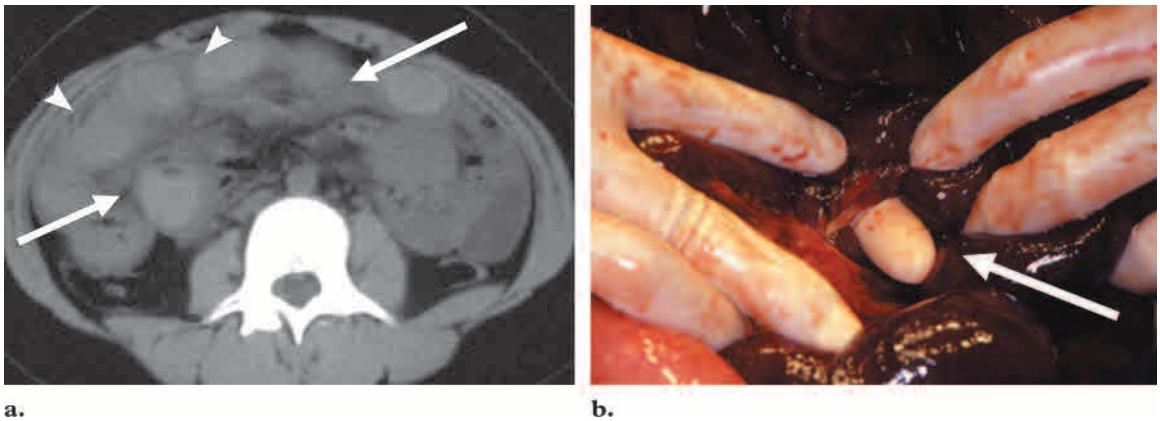

a. b.

Figure 9. Transmesenteric hernia in a 12-year-old girl who experienced 36 hours of diffuse abdominal pain and sudden development of cramps. Abdominal examination showed severe distention and tenderness at the midabdomen. Laboratory investigations revealed a hemoglobin level of 8.4 g/dL. **(a)** Nonenhanced CT scan of the midabdomen shows diffuse mesenteric fluid and haziness (arrows) and mildly dilated small bowel loops. The attenuation of the intraluminal fluid is increased (arrowheads) because red blood cells may have been released in the lumen. Laparotomy was performed 12 hours after CT. **(b)** Intraoperative photograph shows the hernial orifice (arrow), which is 3 cm in diameter. Approximately 260 cm of small intestine, located 100 cm from the ileocecal valve, was herniated through the mesenteric defect and twisted 360°; 230 cm was gangrenous and was thus resected.

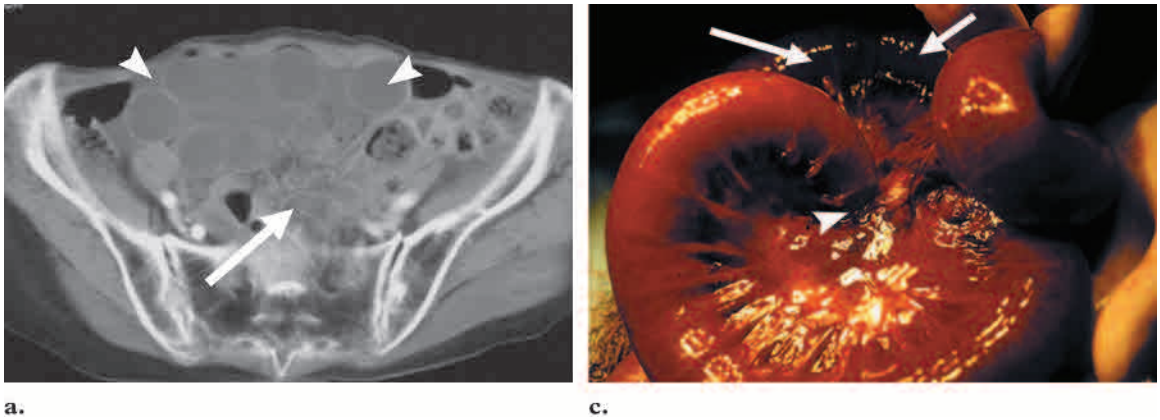

a. c.

Figure 10. Transomental hernia in a 76-year-old woman with a 6-day history of lower abdominal pain. **(a)** Contrast-enhanced CT scan of the pelvis shows a cluster of fluid-filled small bowel loops (arrowheads) with poor or absent enhancement of bowel walls adjacent to the midabdominal wall. The mesenteric vascular pedicle (arrow), which is crowded and engorged with vessels, is observed at the hernial orifice. Laparotomy was performed 3 hours after CT. **(b)** Diagram (coronal view) of the surgical findings shows that the hernial orifice (arrow) is in the periphery of the greater omentum. **(c)** Intraoperative photograph shows the hernial orifice (arrowhead). Approximately 80 cm of ileum, located 70 cm from the ileocecal valve, was herniated through the defect; 55 cm was resected due to gangrene (arrows).

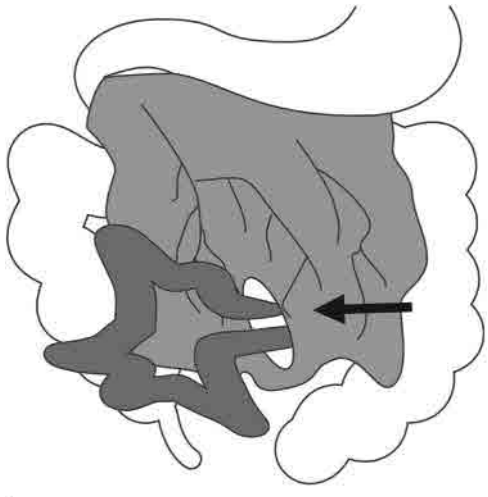

b.

differentiate closed-loop obstructions caused by herniation through the mesenteric defect from those caused by prolapse of the intestine under adhesive bands. A volvulus may further complicate the process and cause rapid hernial strangulation and intestinal gangrene (Fig 9) (1,3,32). A transmesenteric hernia usually manifests in asso-

Figure 11. Transomental hernia in a 78-year-old man with acute epigastric pain of 24 hours duration. At admission, the vital signs, laboratory values, and results of physical examination were normal with the exception of mild epigastric pain. On the second hospital day, laboratory investigations showed a white blood cell count of 20,300/mm^3 (20.3 × 10^9/L). **(a)** Contrast-enhanced CT scan of the midabdomen shows dilated and fluid-filled closed bowel loops *(S)* surrounded by massive ascites (arrowheads). Engorged and crowded mesenteric vessels (arrow) are seen at the hernial orifice, which is adjacent to the abdominal wall. Laparotomy was performed 2 hours after CT. **(b)** Diagram (coronal view) of the surgical findings shows that the hernial orifice (arrow) is 3 cm in diameter with a firm and fibrous edge. **(c)** Intraoperative photograph shows approximately 90 cm of gangrenous jejunal loops (arrows), located 120 cm from the Treitz ligament, which were resected.

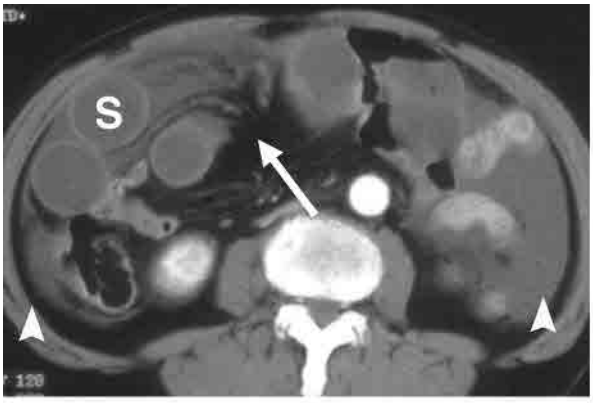

a.

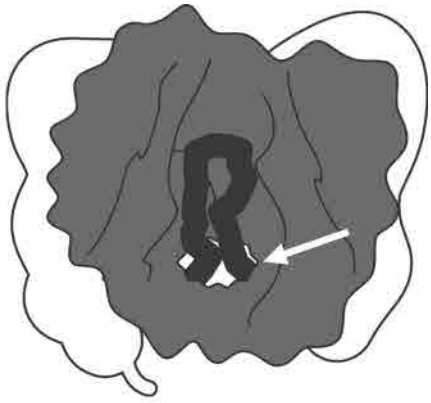

b.

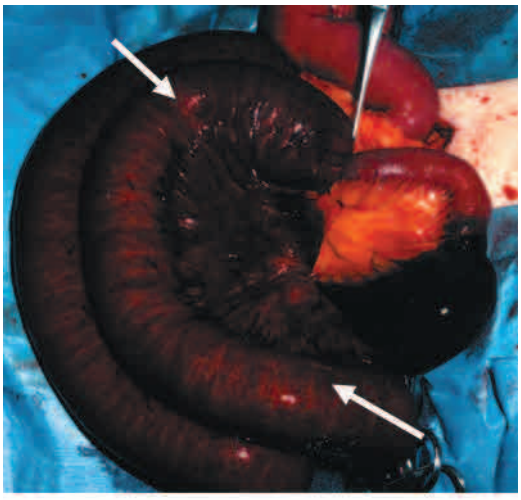

c.

ciation with proximal small bowel dilatation, with a transition zone to a normal or collapsed intestine. Because the bowel mesenteric defect itself is not visualized, observation of the clustering of small bowel loops and abnormalities of the mesenteric vessels plays an important role in diagnosis of transmesenteric hernia. CT shows that the mesenteric vascular pedicle is characteristically engorged, stretched, and crowded; in addition, converging mesenteric vessels are located at the entrance of the hernial sac (34) and there is displacement of the main mesenteric trunk (9,10,32).

Transomental Hernia

Transomental hernias constitute approximately 1%–4% of all internal hernias. There are two types: In the first type, herniation occurs through a free greater omentum; this type is more common, and no sac is present. In the second type, which is rare, herniation into the lesser sac occurs through the gastrocolic ligament (33,35,36).

In the first type, the hernial orifice on the greater omentum is located in the periphery near the free edge (Fig 10) and is usually a slitlike opening from 2 to 10 cm in diameter (1–4,37). The cause of the omental defect has not been identified, but it has been suggested that most have a congenital origin, although inflammation, trauma, and circulation may also cause omental perforations. Small bowel loops, the cecum, and the sigmoid colon are involved in this defect. The clinical and radiologic findings are almost identical to those of transmesenteric hernias (Fig 11) (1,3,38).

Pericecal Hernia

Anatomy

Embryologically, the anatomy of the cecal and pericecal peritoneum is not determined until the 5th fetal month, when the migration of the midgut

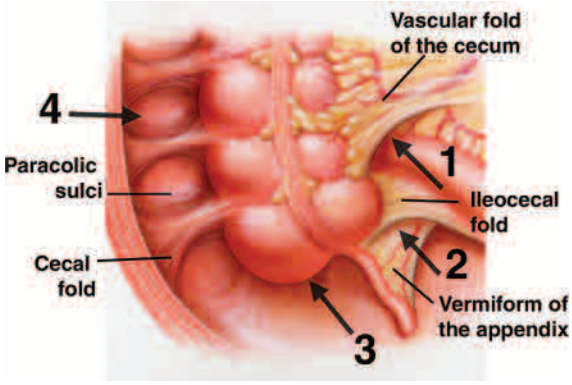

Figure 12. Drawing (coronal view) shows the locations of pericecal recesses. *1* = superior ileocecal recess, *2* = inferior ileocecal recess, *3* = retrocecal recess, *4* = paracolic sulci. (Adapted and reprinted, with permission, from reference 41.)

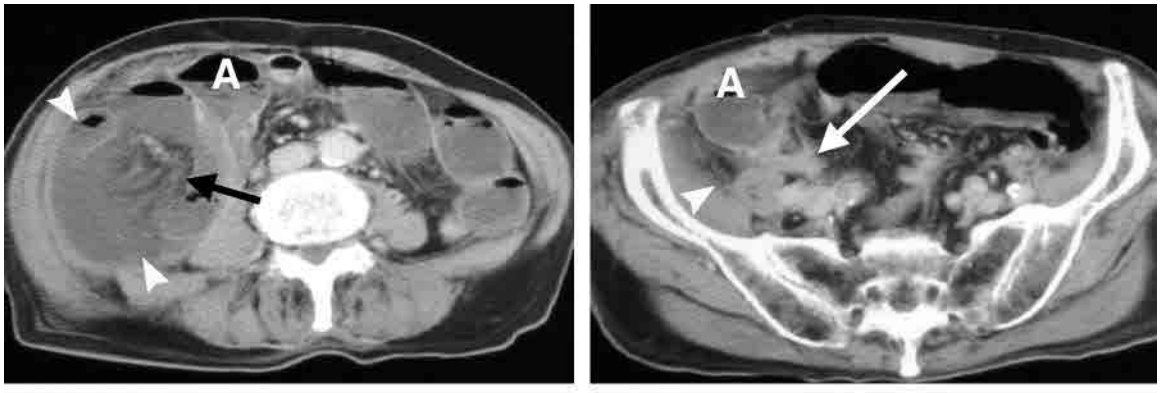

a. **b.**

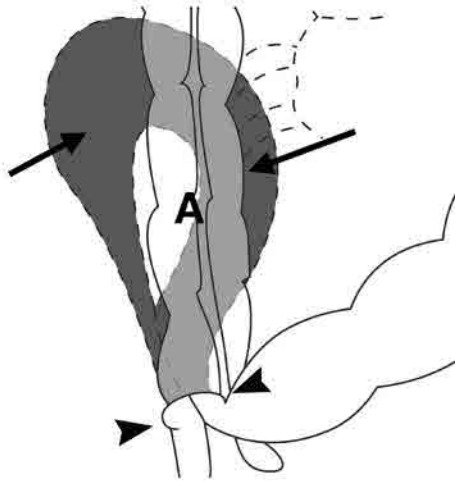

c.

Figure 13. Pericecal hernia through the retrocecal recess in an 84-year-old man with colicky right lower quadrant pain and vomiting of 48 hours duration. He underwent an appendectomy at 54 years of age. **(a)** Contrast-enhanced CT scan of the midabdomen shows a cluster of encapsulated small bowel loops (arrowheads) in the lateral aspect of the right paracolic gutter and behind the ascending colon *(A)*. Dilated and stretched mesenteric vessels (arrow) are seen within the cluster. **(b)** CT scan of the lower abdomen shows beaking and collapsed bowel loops (arrow) at the retrocecal recess (arrowhead). The ascending colon *(A)* is displaced anteriorly. Laparotomy was performed 12 hours after CT. **(c)** Diagram (coronal view) of the surgical findings shows that approximately 230 cm of gangrenous jejunum and ileum (arrows), located 120 cm from the ligament of Treitz, was herniated through the retrocecal recess (arrowheads). The gangrenous bowel loops were resected. *A* = ascending colon.

is complete, with the cecum fixed in the right colic fossa and resorption of the peritoneal surfaces (39,40). Four different pericecal recesses formed by folds of the peritoneum have been reported: the superior ileocecal recess, inferior ileocecal recess, retrocecal recess, and paracolic sulci (Fig 12) (3,39,40,42).

The superior ileocecal recess is bounded in front by the vascular fold of the cecum and behind by the ileal mesentery. The inferior ileocecal recess is bounded in front by the ileocecal fold, above by the posterior ileal surface and its mesentery, to the right by the cecum, and behind by the upper mesoappendix (22). The retrocecal recess, the largest of the four recesses, is bounded anteriorly by the posterior wall of the cecum, posteriorly by the posterior abdominal wall, superiorly by the reflection of the visceral peritoneum coating the posterior wall of the cecum, and medially and laterally by two cecal folds of the peritoneum (40). Paracolic sulci are lateral depressions of the peritoneum investing the cecum. These recesses may be absent or rarely extend posterior to the cecum, forming pockets large enough to admit several fingers (42).

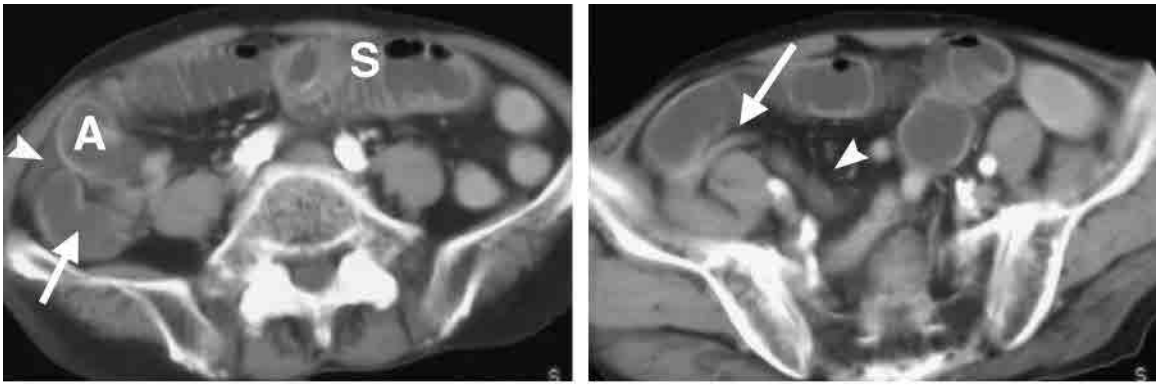

a. b.

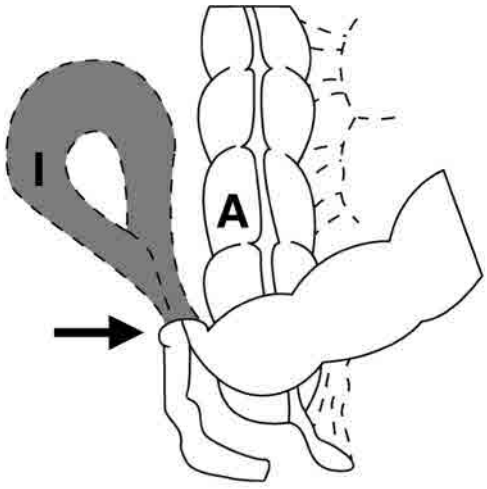

c.

Figure 14. Pericecal hernia through the paracolic sulci in an 86-year-old man with a 10-day history of lower abdominal pain and vomiting. He underwent an appendectomy at 56 years of age. **(a)** Contrast-enhanced CT scan of the lower abdomen shows dilated small bowel loops *(S)* and a cluster of fluid-filled small bowel loops (arrow). The ascending colon *(A)* is displaced anteriorly, and ascites (arrowhead) is seen in the right paracolic gutter. **(b)** CT scan of the pelvis shows that the bowel loops of the oral aspect of the intestine are dilated (arrowhead) and the bowel loops of the anal aspect are collapsed (arrow). Laparotomy was performed 6 hours after CT. **(c)** Diagram (coronal view) of the surgical findings shows that approximately 20 cm of strangulated ileum *(I)*, located 130 cm from the ileocecal valve, was herniated through a 5-cm-diameter defect of the paracolic sulci (arrow); 10 cm of the incarcerated ileum was resected due to gangrenous changes. *A* = ascending colon.

Furthermore, according to the literature (43,44), supplementary recesses and fossae may develop in the ileocecal area because of individual variations in the processes of bowel rotation and peritoneal fusion. These structures may also become hernial orifices.

Features

Pericecal hernias account for 13% of all internal hernias. In most cases, ileal loops herniate through the defect and occupy the right paracolic gutter (Fig 13). Clinical diagnosis is difficult because clinical symptoms and physical examination usually indicate acute SBO, but in chronic incarceration diagnoses are confused with inflammatory bowel disease, appendiceal disorders, or other causes of SBO (4,39). In establishing the precise preoperative diagnosis, delayed radiographs from a small bowel series or barium enema examinations are considered to be helpful when the patient's condition permits these examinations (1,3). The specific CT appearance of a pericecal hernia is not established, and there are few cases in the literature (40,42–44). In our two cases, CT scans demonstrated a cluster of fluid-filled small bowel loops (Fig 14) located lateral to the cecum and posterior to the ascending colon. In addition, a beaking appearance indicative of tethering at the aperture of the peritoneal recess and dilatation of small bowel loops with a transition zone were revealed. On the basis of these CT findings, pericecal hernia can be diagnosed with high certainty (40).

Sigmoid Mesocolon Hernia

Anatomy

The sigmoid mesocolon is a peritoneal fold attaching the sigmoid colon to the pelvic wall. The apex is divided near the left common iliac artery and serves as a potential site for an internal hernia. The intersigmoid fossa (Fig 1, *G*) lies behind this apex of the V-shaped parietal attachment of the sigmoid mesocolon. This pocket is found in 65% of autopsies and varies in size from a dimple to a fossa admitting the fifth finger (1,3,22).

Features

Sigmoid mesocolon hernias account for 6% of all internal hernias (1–3) and are divided into three categories (45): *(a)* intersigmoid hernia,

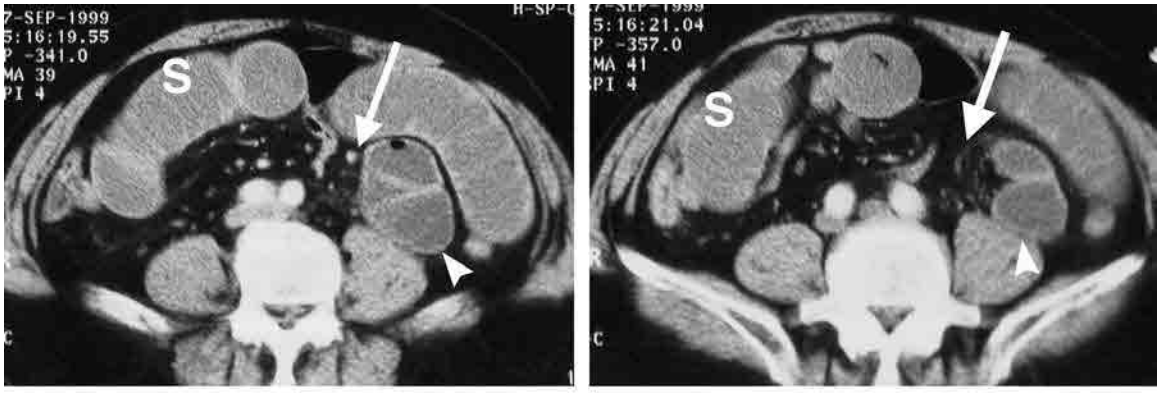

a. b.

Figure 15. Intramesosigmoid hernia in a 79-year-old man with acute lower abdominal pain of 3 hours duration. CT was performed 4 days after conservative treatment with a nasogastric tube. **(a, b)** Contrast-enhanced CT scans of the pelvis (**b** obtained 20 mm below **a**) show multiple dilated small bowel loops *(S)*. A dilated inferior mesenteric vein (arrow) appears as a landmark at the edge of the inferior mesentery. A saclike mass of incarcerated jejunal loops (arrowhead) is located anterior to the left psoas muscle. Laparotomy was performed 4 days after CT. **(c)** Diagram (coronal view) of the surgical findings shows that 20 cm of jejunum *(J)*, located 230 cm from the ligament of Treitz, was herniated into a defect (arrow) on the left side of the sigmoid mesocolon. The defect was 3 cm in diameter and was located in the anterior layer of the left side of the sigmoid mesocolon.

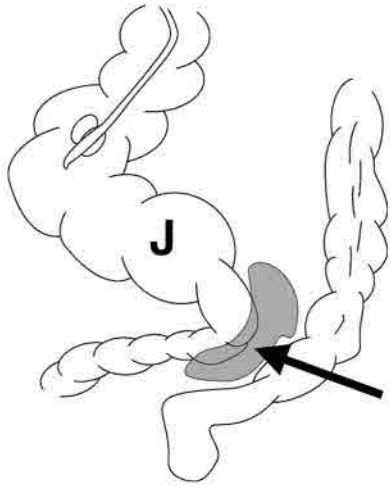

c.

(b) transmesosigmoid hernia, and *(c)* intermesosigmoid hernia. Because preoperative differentiation of the three hernia types involving the sigmoid mesocolon is often difficult, the diagnosis is confirmed only with surgical management in most cases. Intersigmoid hernia, which is the most common type, is herniation into a congenital fossa, the intersigmoid fossa, situated in the attachment of the lateral aspect of the sigmoid mesocolon. Transmesosigmoid hernia is incarceration of small bowel loops through a defect in the sigmoid mesocolon. This defect is oval and ranges in diameter from 2 to 4 cm (1,3,45,46). Transmesosigmoid hernia involves both layers of the sigmoid mesentery and allows herniation of the small bowel loops toward the left lower abdomen, posterior-lateral to the sigmoid colon. This hernia is demonstrated to be without an actual hernial sac (47,48). Intramesosigmoid hernia is incarceration with a hernial sac through a congenital defect, present in only one of the constituent leaves of the sigmoid mesentery (Fig 15) (45).

Supravesical and Pelvic Hernias

The peritoneum follows the surfaces of the pelvic viscera and walls (Fig 2) with differences between the sexes.

Anatomy of the Lesser Pelvis in Males

The peritoneum leaves the junction of the middle and lower third of the rectum and passes forward to the upper poles of the seminal vesicle and the superior aspect of the bladder. Between the rectum and bladder, the peritoneum forms a retrovesical pouch. Lateral to the rectum, the peritoneum forms right and left perirectal fossae, anterior to which is the retrovesical pouch. The anterior peritoneum covers the superior surface of the bladder, forming a paravesical fossa on each side (9).

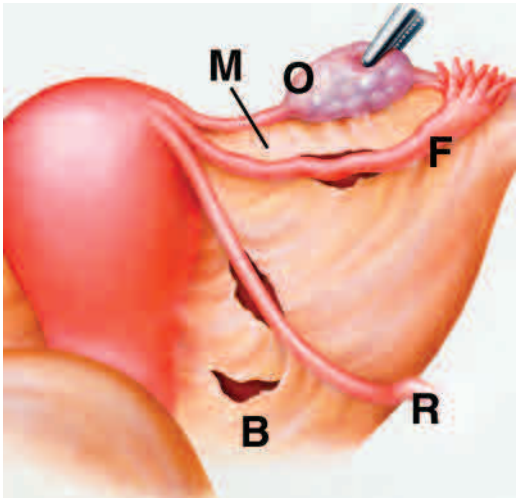

Figure 16. Drawing (coronal view) shows the anatomy of the broad ligament *(B)* and various defects. *F* = fallopian tube, *M* = mesosalpinx, *O* = ovary, *R* = round ligament. (Adapted and reprinted, with permission, from reference 7.)

Supravesical Hernia

The supravesical fossa is the area of the abdominal wall between the remnants of the median and the left or right umbilical ligaments (49). The sac may remain above the pelvis and form an external supravesical hernia or pass downward and form an internal supravesical hernia. Internal supravesical hernias are divided into the following three categories: *(a)* anterior, *(b)* right or left lateral, and *(c)* posterior, which are based on whether the course is in front of, beside, or behind the bladder (50).

Anatomy of the Lesser Pelvis in Females

Perirectal and paravesical fossae also appear in females. At the lateral limit of the paravesical fossae, the peritoneum invests the mesosalpinx, round ligament, and broad ligament of the uterus. The rectovesical pouch is divided by the uterus and vagina into the vesicouterine pouch and rectouterine pouch (pouch of Douglas). The broad ligaments extend from the sides of the uterus to the lateral pelvic walls (Fig 16). The superior extent of the broad ligaments contains the fallopian tubes. Immediately below the fallopian tubes, the anterior and posterior peritoneal folds condense to form the mesosalpinx. The mesosalpinx is bounded by the fallopian tube superiorly, the uterus medially, the ovary laterally, and the ovarian ligament inferiorly. The lateral extent of the broad ligament covers the ovarian vessels, forming the infundibulopelvic ligament, which suspends the ovary. The anterior leaf of the broad ligament covers the round ligament of the uterus and forms the mesoligamentum teres (9,51).

Hernia through the Broad Ligament

Hernias through a defect of the broad ligament account for only 4%–5% of all internal hernias (1,3,52). The herniated viscus is the small intestine in more than 90% of cases. The typical patient with this hernia is a middle-aged woman who has been pregnant and has no history of abdominal surgery. More than 85% of these hernias have occurred in parous women (51).

Broad ligament defects are classified as congenital or acquired. Congenital cases have an embryologic basis due to a developmental peritoneal defect around the uterus. Acquired defects are due to surgical trauma, pregnancy and birth trauma, perforations following vaginal manipulation, and prior pelvic inflammatory disease (52). A classification for the broad ligament has been proposed on the basis of the anatomic position of the defect: type 1 = defect caudal to the round ligament, type 2 = defect above the round ligament, and type 3 = defect between the round ligament and the remainder of the broad ligament through the mesoligamentum teres (53).

On the other hand, Hunt (54) classified two types of hernia through the broad ligament. One is the fenestra type, through a defect in the broad ligament, and the other is the pouch type, with herniation into an anterior or posterior aperture of the broad ligament. The fenestra type, with complete defects, may allow passage of small bowel loops with potential hernial strangulation. These are the most common cases. The pouch type, with single-layer defects, may allow visceral structures to enter and become entrapped in the parametrial tissue (54,55). The following are the characteristic CT appearances (56): *(a)* a cluster of dilated small bowel loops with air-fluid levels in

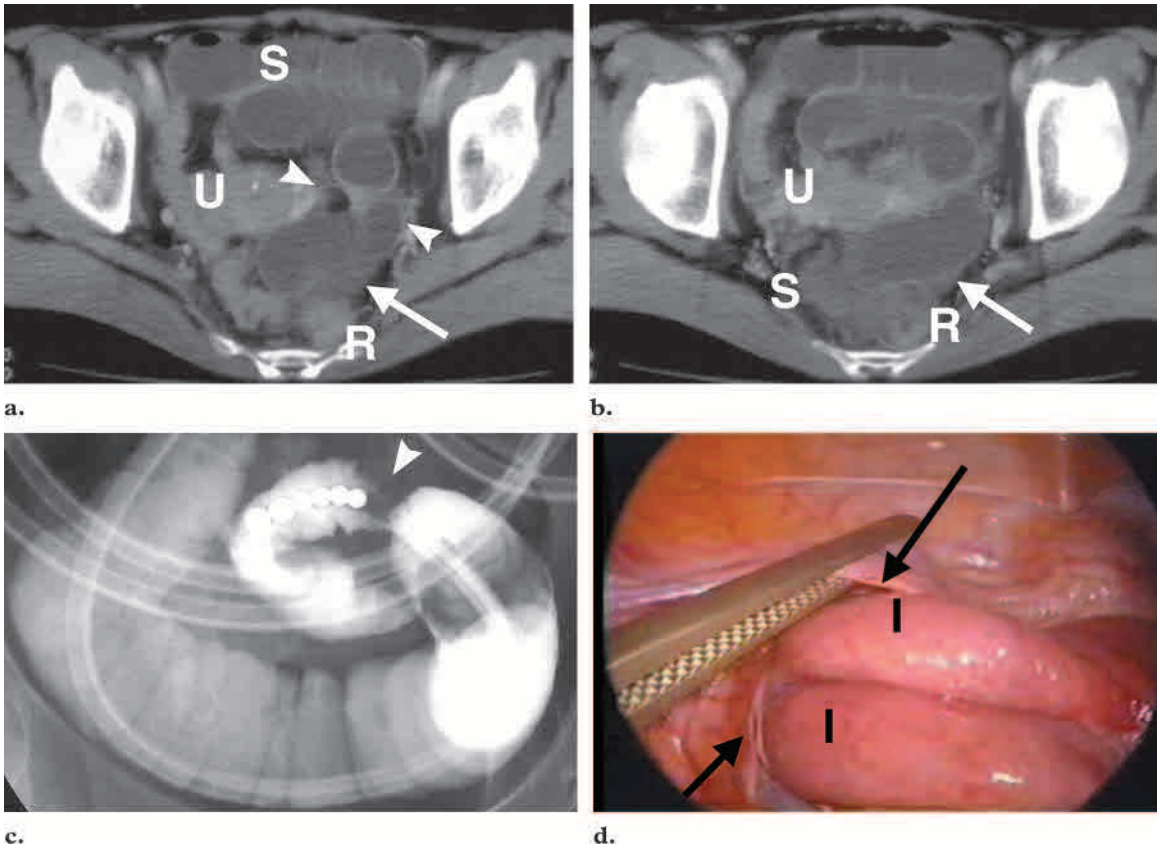

Figure 17. Hernia through the broad ligament in a 51-year-old woman, gravida 2, para 2, with acute lower abdominal pain of 24 hours duration. She had no significant medical history. **(a)** Contrast-enhanced CT scan of the pelvis shows dilated small bowel loops *(S)* and a cluster of dilated bowel loops with air-fluid levels (arrow) between the uterus *(U)* and rectum *(R)*. Stenosis of an incarcerated bowel loop (arrowheads) can be visualized because of the fat layer around the uterus; the C-shaped configuration of the bowel loop suggests a closed-loop obstruction. **(b)** CT scan obtained 10 mm below **a** shows that the rectum *(R)* and sigmoid colon *(S)* are compressed dorsolaterally and the uterus *(U)* is compressed ventrally. Arrow = cluster of dilated bowel loops. **(c)** Image obtained with enteroclysis performed through a long intestinal tube shows an SBO (arrowhead). Laparotomy was performed 11 days after CT. **(d)** Laparoscopic photograph shows viable distal ileal loops *(I)* herniated from anterior to posterior through a defect in the left broad ligament (arrows). Resection was not performed.

the pelvic cavity and *(b)* bowel loops compressing the rectosigmoid dorsolaterally and the uterus ventrally (Fig 17).

Hernia through the Perirectal Fossa

We found no reports of internal hernias through a defect of the perirectal fossa and only three reports of internal hernias through the pouch of Douglas in the English-language literature (57–59). The pouch of Douglas is a peritoneal reflection between the uterus and the rectum, and its depth varies extensively; an abnormally deep pouch of Douglas may lead to a posterior perineal hernia (59,60). These defects are believed to be congenital without abnormality of the pouch of Douglas or the pelvic floor musculature. In our patient, approximately two-thirds of the circumference of the antimesenteric ileal wall was involved through a defect of the right perirectal fossa in a Richter hernia (Fig 18). This peritoneal defect was also believed to be congenital without abnormality of the perirectal fossa or the pelvic floor musculature.

Relationship of CT Findings to Clinical Findings and Management

Internal hernias are uncommon and are rarely preoperatively diagnosed because there are no specific clinical symptoms. The most common clinical presentation is bowel ischemia with some degree of SBO. However, if hernias are easily reducible, the clinical presentation may be intermittent or transient. During asymptomatic intervals, clinical or radiologic studies may reveal no abnormality (9,10).

In acute-onset and high-grade SBO, some investigators have recommended direct surgical exploration, whereas partial obstruction can initially be managed with conservative treatment

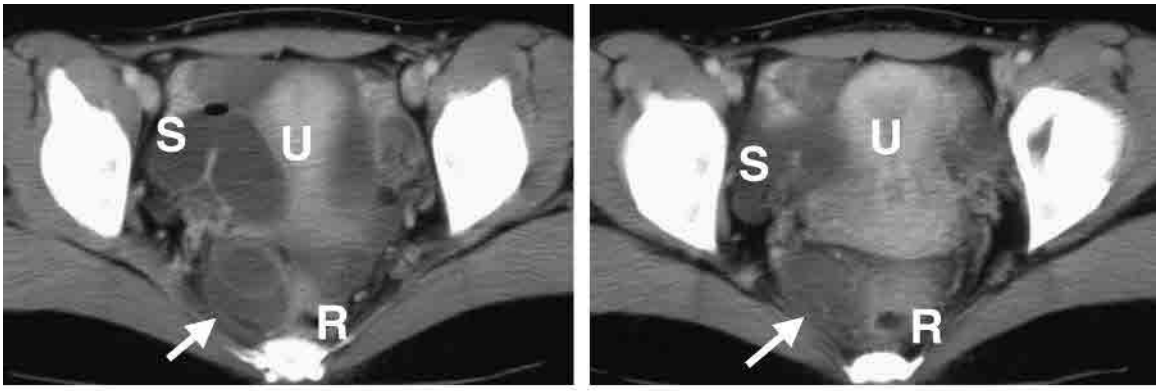

a. b.

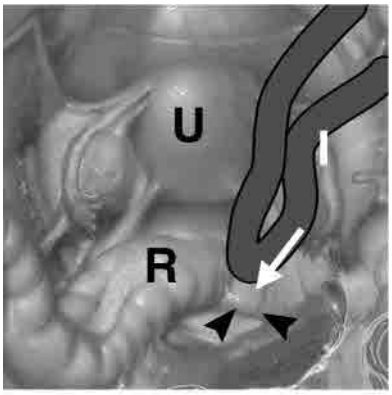

c.

Figure 18. Hernia through a defect of the right perirectal fossa in a 28-year-old woman with continuous lower abdominal pain of 34 hours duration. **(a, b)** Contrast-enhanced CT scans of the pelvis (**b** obtained 10 mm below **a**) show dilated and fluid-filled small bowel loops *(S)*. A cluster of dilated bowel loops (arrow) is located to the right of the rectum *(R)* and behind the uterine cervix *(U)*. Laparotomy was performed 4 hours after CT. **(c)** Drawing (superior view) of the surgical findings shows that the antimesenteric wall of an ileal loop *(I)*, located 50 cm from the ileocecal valve, was herniated (Richter hernia) through a defect (arrow) in the anterior peritoneal layer of the right perirectal fossa (arrowheads). When withdrawn manually, the incarcerated bowel loop was viable and nongangrenous. *R* = rectum, *U* = uterus.

(4,11,12). Nevertheless, even if the affected bowel loops at the abnormal anatomic location are not dilated and small internal hernias with low-grade obstruction are detected, we recommend that surgical colleagues use appropriate care to decrease hernial strangulation. Examples of such care include carefully monitoring the patient's vital signs and physical examination results or performing follow-up CT or gastrointestinal studies enhanced with intraluminal contrast material, including CT enteroclysis.

Conclusions

Understanding the anatomy of the peritoneal cavity and the characteristic anatomic location of each internal hernia, as well as recognition of the characteristic CT findings, may assist in consideration or identification of internal hernias in most cases of SBO. Currently, multi–detector row CT is most often recommended to detect the cause of SBO and to facilitate diagnosis of a variety of internal hernias. Therefore, appropriate guidance of surgical colleagues by radiologists may be essential to avoid irreversible damage to the bowel wall and mesentery.

Acknowledgments: We express our sincere thanks to Mika Yamamoto, DDS, and Tsukasa Sano, DDS, for their cooperation in preparation of the manuscript and their helpful advice.

References

1. Mayers MA. Internal abdominal hernias. In: Mayers MA, ed. Dynamic radiology of the abdomen. 5th ed. New York, NY: Springer-Verlag, 2000; 711–748.
2. Ghahremani GG. Internal abdominal hernias. Surg Clin North Am 1984; 64:393–406.
3. Ghahremani GG. Abdominal and pelvic hernias. In: Gore RM, Levine MS, eds. Textbook of gastrointestinal radiology. 2nd ed. Philadelphia, Pa: Saunders, 2000; 1993–2009.
4. Newsom BD, Kukora JS. Congenital and acquired internal hernias: unusual causes of small bowel obstruction. Am J Surg 1986; 152:279–285.
5. Zarvan NP, Lee FT Jr, Yandow DR, Unger JS. Abdominal hernias: CT findings. AJR Am J Roentgenol 1995; 164:1391–1395.
6. Asanuma Y. Pancreas and spleen. In: Matsuno S, Hatakeyama K, Kanematsu T, eds. Comprehensive anatomy for gastroenterological surgery: small intestine, anorectal disease, colon, liver, gallbladder, biliary tract, pancreas and spleen. Tokyo, Japan: Medical View, 1999; 108–144.
7. Kudo M. Operation for uterus. In: Takeda Y, ed. Anatomy for obstetric and gynecologic surgery. Tokyo, Japan: Medical View, 1999; 38–67.
8. Welch CE. Hernia: intestinal obstruction. Chicago, Ill: Year Book Medical, 1958; 239–268.
9. Blachar A, Federle MP, Dodson SF. Internal hernia: clinical and imaging findings in 17 patients with emphasis on CT criteria. Radiology 2001; 218:68–74.
10. Blachar A, Federle MP, Brancatelli G, Peterson MS, Oliver JH 3rd, Li W. Radiologist perfor-

mance in the diagnosis of internal hernia by using specific CT findings with emphasis on transmesenteric hernia. Radiology 2001; 221:422–428.
11. Herlinger H, Rubesin SE, Morris JB. Small bowel obstruction. In: Gore RM, Levine MS, eds. Textbook of gastrointestinal radiology. 2nd ed. Philadelphia, Pa: Saunders, 2000; 815–837.
12. Furukawa A, Yamasaki M, Furuichi K. Helical CT in the diagnosis of small bowel obstruction. RadioGraphics 2001; 21:341–355.
13. Horton KM, Fishman EK. The current status of multidetector row CT and three-dimensional imaging of the small bowel. Radiol Clin North Am 2003; 41:199–212.
14. Maglinte DD, Bender GN, Heitkamp DE, Lappas JC, Kelvin FM. Multidetector-row helical CT enteroclysis. Radiol Clin North Am 2003; 41:249–262.
15. Chou CK. CT manifestations of bowel ischemia. AJR Am J Roentgenol 2002; 178:87–91.
16. Balthazar EJ, Liebeskind ME, Macari M. Intestinal ischemia in patients in whom small bowel obstruction is suspected: evaluation of accuracy, limitations, and clinical implications of CT in diagnosis. Radiology 1997; 205:519–522.
17. Rha SE, Ha HK, Lee SH, et al. CT and MR imaging findings of bowel ischemia from various primary causes. RadioGraphics 2000; 20:29–42.
18. Obuz F, Terzi C, Sokmen S, Yilmaz E, Yildiz D, Fuzun M. The efficacy of helical CT in the diagnosis of small bowel obstruction. Eur J Radiol 2003; 48:299–304.
19. Wiesner W, Khurana B, Ji H, Ros PR. CT of acute bowel ischemia. Radiology 2003; 226:635–650.
20. Hanssmann GH, Morton SA. Intraabdominal hernia. Arch Surg 1939; 39:973–986.
21. Sufian S, Matsumoto T. Intestinal obstruction. Am J Surg 1975; 130:9–14.
22. Bannister LH. Alimentary system. In: Williams PL, ed. Gray's anatomy. 38th ed. New York, NY: Churchill Livingstone, 1995; 1683–1812.
23. Miller PA, Mezwa DG, Feczko PJ, Jafri ZH, Madrazo BL. Imaging of abdominal hernias. RadioGraphics 1995; 15:333–347.
24. Vint WA. Herniation of the gallbladder through the epiploic foramen into the lesser sac: radiologic diagnosis. Radiology 1966; 86:1035–1040.
25. Wojtasek DA, Codner MA, Nowak EJ. CT diagnosis of cecal herniation through the foramen of Winslow. Gastrointest Radiol 1991; 16:77–79.
26. Schuster MR, Tu RK, Scanlan KA. Caecal herniation through the foramen of Winslow: diagnosis by computed tomography. Br J Radiol 1992; 65: 1047–1048.
27. Brigham RA. Paraduodenal hernia. In: Nyhus LM, Conden RE, eds. Hernia. 4th ed. Philadelphia, Pa: Lippincott, 1995; 485–490.
28. Berardi RS. Paraduodenal hernias. Surg Gynecol Obstet 1981; 152:99–110.
29. Donnelly LF, Rencken IO, deLorimier AA, Gooding CA. Left paraduodenal hernia leading to ileal obstruction. Pediatr Radiol 1996; 26:534–536.
30. Okino Y, Kiyosue H, Mori H, et al. Root of the small-bowel mesentery: correlative anatomy and CT features of pathologic conditions. RadioGraphics 2001; 21:1475–1490.
31. Olazabal A, Guasch I, Casas D. CT diagnosis of nonobstructive left paraduodenal hernia. Clin Radiol 1992; 46:288–289.
32. Stone AM, Janin Y, Wise L. Mesenteric hernia. In: Nyhus LM, Conden RE, eds. Hernia. 4th ed. Philadelphia, Pa: Lippincott, 1995; 467–474.
33. Takagi Y, Yasuda K, Nakada T, Abe T, Matsuura H, Saji S. A case of strangulated transomental hernia diagnosed preoperatively. Am J Gastroenterol 1996; 91:1659–1660.
34. Mori H. Imaging of mesenteric volvulus and internal hernia of the abdomen; current status. Jpn J Diagn Imaging 1997; 17:276–283.
35. Inoue Y, Nakamura H, Mizumoto S, Akashi H. Lesser sac hernia through the gastrocolic ligament: CT diagnosis. Abdom Imaging 1996; 21:145–147.
36. Masuda H, Nakayama H, Nakamura Y, Aoki N. A rare type of lesser sac hernia. Hepatogastroenterology 2001; 48:741–742.
37. Hull JD 3rd. Transomental hernia. Am Surg 1976; 42:278–284.

38. Delabrousse E, Couvreur M, Saguet O, Heyd B, Brunelle S, Kastler B. Strangulated transomental hernia: CT findings. Abdom Imaging 2001; 26: 86–88.
39. Rivkind AI, Shiloni E, Muggia-Sullam M, Weiss Y, Lax E, Freund HR. Paracecal hernia: a cause of intestinal obstruction. Dis Colon Rectum 1986; 29:752–754.
40. Lu HC, Wang J, Tsang YM, Tseng HS, Li YW. Pericecal hernia: a report of two cases and survey of the literature. Clin Radiol 2002; 57:855–858.
41. Hatakeyama K. Small intestine and colon. In: Matsuno S, Hatakeyama K, Kanematsu T, eds. Comprehensive anatomy for gastroenterological surgery: small intestine, anorectal disease, colon, liver, gallbladder, biliary tract, pancreas and spleen. Tokyo, Japan: Medical View, 1999; 2–69.
42. Bass J Jr, Longley BJ. Paracecal hernia: case report and review of the literature. Am Surg 1976; 42: 285–288.
43. Omori H, Asahi H, Inoue Y, Irinoda T, Saito K. Laparoscopic paracecal hernia repair. J Laparoendosc Adv Surg Tech A 2003; 13:55–57.
44. Lindsey I, Nottle PD. Laparoscopic management of small bowel obstruction caused by a retrocaecal hernia. Surg Laparosc Endosc 1997; 7:349–350.
45. Benson JR, Killen DA. Internal hernias involving the sigmoid mesocolon. Ann Surg 1964; 159:382–384.
46. Yip AW, Tong KK, Choi TK. Mesenteric hernias through defects of the mesosigmoid. Aust N Z J Surg 1990; 60:396–399.
47. Sasaki T, Sakai K, Fukumori D, Sato M, Ohmori H, Yamamoto F. Transmesosigmoid hernia: report of a case. Surg Today 2002; 32:1096–1098.
48. Yu CY, Lin CC, Yu JC, Liu CH, Shyu RY, Chen CY. Strangulated transmesosigmoid hernia: CT diagnosis. Abdom Imaging 2004; 29:158–160.
49. Sasaya T, Yamaguchi A, Isogai M, Harada T, Kaneoka Y, Suzuki M. Supravesical hernia: CT diagnosis. Abdom Imaging 2001; 26:89–91.
50. Skandalakis PN, Skandalakis LJ, Gray SW, Skandalakis JE. Supravesical hernia. In: Nyhus LM, Conden RE, eds. Hernia. 4th ed. Philadelphia, Pa: Lippincott, 1995; 400–411.
51. Slezak FA, Schlueter TM. Hernia of the broad ligament. In: Nyhus LM, Conden RE, eds. Hernia. 4th ed. Philadelphia, Pa: Lippincott, 1995; 491–496.
52. Simstein NL. Internal herniation through a defect in the broad ligament. Am Surg 1987; 53:258–259.
53. Cilley R, Poterack K, Lemmer J, Dafoe D. Defects of the broad ligament of the uterus. Am J Gastroenterol 1986; 81:389–391.
54. Hunt AB. Fenestra and pouches in the broad ligament as an actual and potential cause of strangulated intraabdominal hernia. Surg Gynecol Obstet 1934; 58:906–913.
55. Ishihara H, Terahara M, Kigawa J, Terakawa N. Strangulated herniation through a defect of the broad ligament of the uterus. Gynecol Obstet Invest 1993; 35:187–189.
56. Suzuki M, Takashima T, Funaki H, et al. Radiologic imaging of herniation of the small bowel through a defect in the broad ligament. Gastrointest Radiol 1986; 11:102–104.
57. Fiirgaard B, Agertoft A. Internal Richter's hernia due to congenital peritoneal defect: case report. Acta Chir Scand 1988; 154:537.
58. Inoue Y, Shibata T, Ishida T. CT of internal hernia through a peritoneal defect of the pouch of Douglas. AJR Am J Roentgenol 2002; 179:1305–1306.
59. Hoeffel JC, Zimberger J, Pocard B, Hoeffel C. Demonstration by computed tomography of a case of internal small bowel herniation. Br J Radiol 1992; 65:1045–1046.
60. Baessler K, Schuessler B. The depth of the pouch of Douglas in nulliparous and parous women without genital prolapse and in patients with genital prolapse. Am J Obstet Gynecol 2000; 182:540–544.

This article meets the criteria for 1.0 credit hour in category 1 of the AMA Physician's Recognition Award. To obtain credit, see accompanying test at http://www.rsna.org/education/rg_cme.html.